Study of the Z-dependence of core impurity transport in LHD plasmas by means of a new type of TESPEL

N. Tamura[1,2], M. Yoshinuma[1], K. Ida[1,2], C. Suzuki[1,2],
M. Goto[1,2], T. Oishi[1,2], M. Shoji[1], K. Mukai[1,2], H. Funaba[1]

[1]National Institute for Fusion Science, NINS, Toki, Japan
[2]SOKENDAI (The Graduate University for Advanced Studies), Toki, Japan

Introduction At present, problems regarding impurities in magnetically-confined fusion (MCF) plasmas are becoming more complex because various impurities will exist simultaneously inside a high-temperature MCF plasma. In general, the transport of heat and particles in MCF plasmas is determined mainly by turbulent transport. However, for impurities with a high Z number, a contribution of neoclassical transport may not be negligible. An outstanding example of the contribution of neoclassical transport is an impurity accumulation where the impurities accumulate in the centre of the MCF plasmas. Therefore, investigating the Z-dependence of core impurity transport in the MCF plasma will help us to understand the interaction between turbulent and neoclassical transport in impurity transport. In LHD, we investigated the dependence of core impurity transport on an atomic number (Z) with a new type of TESPEL. The TESPEL method can exclude the influence of the SOL on the impurity transport study in the confined plasma owing to its unique feature. And thus, the TESPEL allows us to investigate more clearly the impurity transport in the core plasma of LHD.

Experimental setup More recently, for studying simultaneously the behaviours of low- and mid/high-Z impurities in the MCF plasmas, a new type of TESPEL [1], which contains an inorganic compound, has been developed and its ability has been demonstrated [2]. For instance, the TESPEL containing a lithium titanate (Li_2TiO_3) can be utilized for measuring the behaviours of lithium (Li), oxygen (O) and titanium (Ti) impurities simultaneously. In this study, the TESPELs containing lithium titanate (Li_2TiO_3: Z=3, 22 and 8), silicon hexaboride (SiB_6: Z=14, 5), sodium chloride (NaCl: Z = 11, 17), and calcium aluminate ($CaAl_2O_4$: Z = 20, 13 and 8), were utilized. Here, the outer shell of TESPEL is made of polystyrene (-$CH(C_6H_5)CH_2$-). And the outer diameter and shell thickness of the TESPELs is about 900 μm and 120 μm, respectively. The TESPELs containing the compound tracers were injected into the LHD plasma through a straight-line of a double-barreled TESPEL injector, which was more recently installed at the Port 3-O of LHD [3]. Line emissions from the highly ionized impurities derived from the TESPEL were measured basically with EUV/VUV spectrometers. Further, the spatio-temporal behaviours of some of those impurities were measured by using a charge exchange spectroscopy (CXS) technique.

Experimental results and discussions The Z dependence of core impurity transport in LHD plasmas was investigated in both low- and high-density regimes. Figure 1 shows a plasma waveform summary for four(4) low-density (a line-averaged electron density n_{e_bar} of around 2 x 10^{19} m^{-3}) LHD plasmas, #169088: SiB_6 (orange), #169090: NaCl (light blue), #169092: $CaAl_2O4$ (blue), #169094: Li_2TiO_3 (red). As can be recognized easily, the target plasmas with the low-density are almost identical. The TESPEL was injected at the time of around 3.875 s as indicated by a vertical dashed line in Fig.1. After the TESPEL injection, the line-averaged electron density was slightly increased. Then the elevated line-averaged electron density was decreased to the pre-injection level except for the case with the SiB_6-TESPEL. This could be because the amount of SiB_6 tracer is slightly higher than the other tracers. The central electron temperature T_{e0} was also increased around the time of TESPEL injection, but the T_{e0} increment

was due to the addition of NBI#4 and NBI#5, not due to the TESPEL injection. Here, NBI#5 is used as a probe beam for the CXS technique. Figure 2 (a-c) shows temporal evolutions of the charge exchange (CX) Li III, CX B V and CX Al XIII emissions measured with the CXS technique in the low-density plasmas. Here, these temporal evolutions are obtained by integrating over all the spatial channel data of CXS diagnostic. As can be seen, all the CX emissions were increased clearly in response to the TESPEL injection. Decay times of CX emissions from Li, B, and Al ions, which can be considered as a global impurity transport time, seem to increase with the atomic number. Figure 2 (d-g) shows temporal evolutions of Li-like emissions from Si, Cl, Ca, and Ti ions introduced by the TESPEL. Here, the Li-like emissions were measured with the SOXMOS spectrometer installed at the Port 7-O of the LHD and those emissions were normalized by the maximum during the period shown. Decay times of Li-like emissions from highly-ionized Si, Cl, Ca, Ti impurities can be also considered as a global impurity transport time, because the SOXMOS spectrometer can measure sight-volume

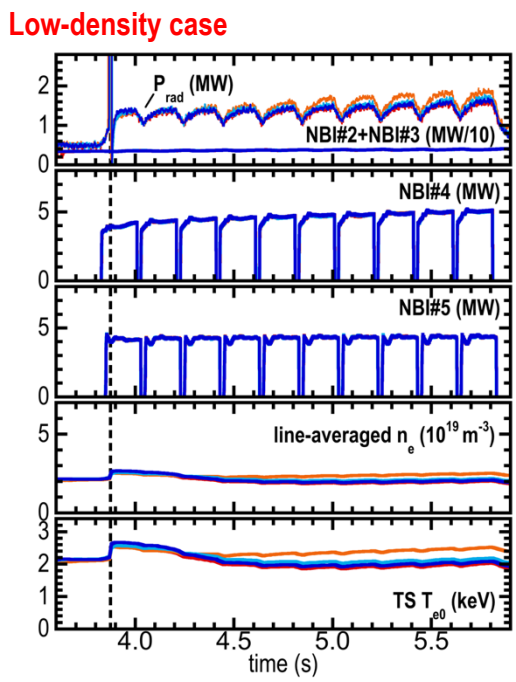

Fig.1. Plasma waveform summary for 4 low-density LHD plasmas, #169088: SiB_6 (orange), #169090: NaCl (light blue), #169092: $CaAl_2O_4$ (blue), #169094: Li_2TiO_3 (red).

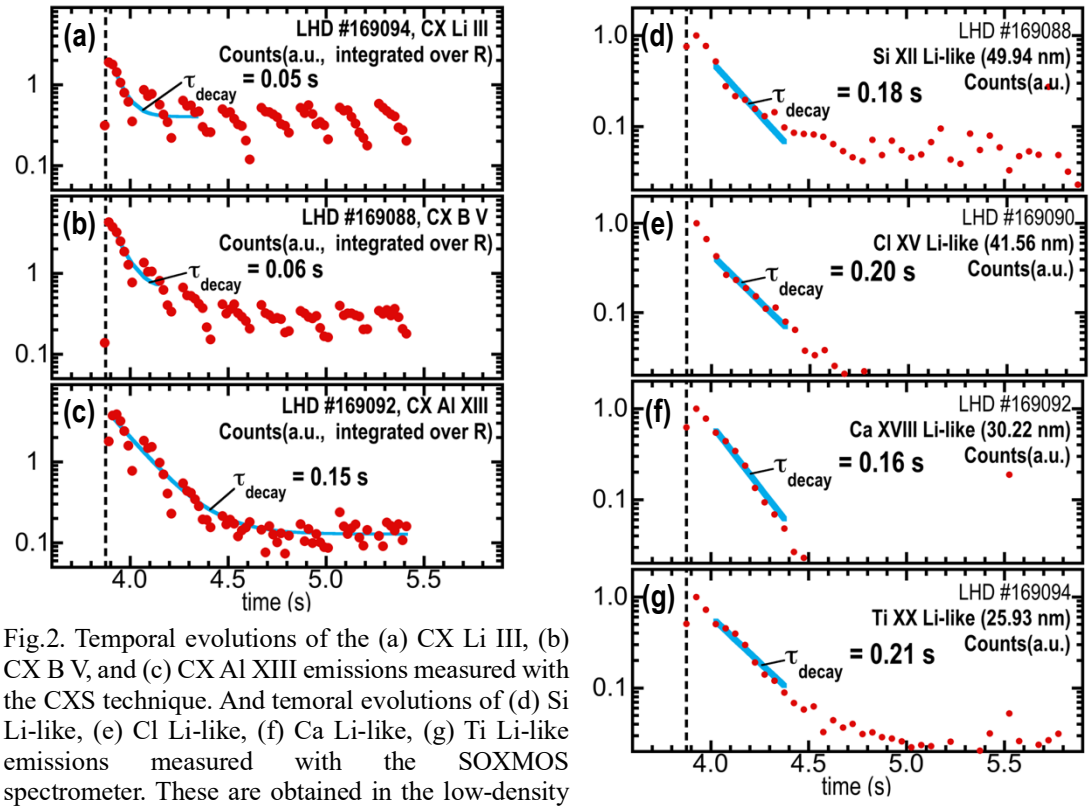

Fig.2. Temporal evolutions of the (a) CX Li III, (b) CX B V, and (c) CX Al XIII emissions measured with the CXS technique. And temoral evolutions of (d) Si Li-like, (e) Cl Li-like, (f) Ca Li-like, (g) Ti Li-like emissions measured with the SOXMOS spectrometer. These are obtained in the low-density LHD plasmas.The vertical dashed line indicates the TESPEL injection time. All the Li-like emissions are normalized by the maximum druing the time period shown.

integrated EUV/VUV spectra. The decay times of Si, Cl, Ca, and Ti Li-like emissions seem not to be much different from each other.

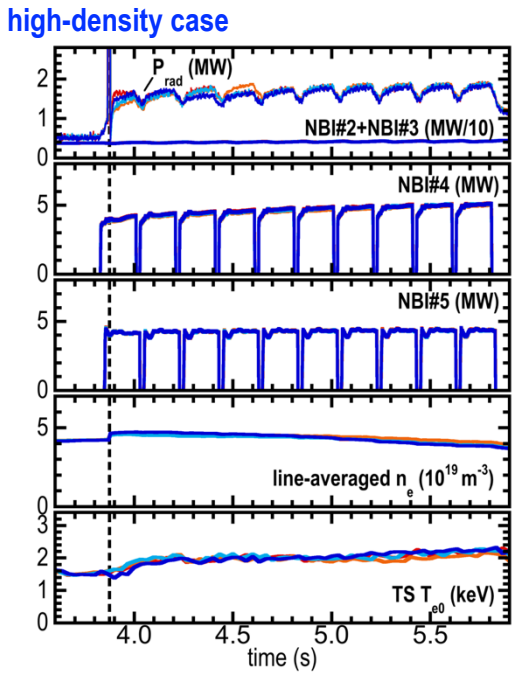

Fig.3. Plasma waveform summary for 4 high-density LHD plasmas, #169063: SiB_6 (orange), #169067: NaCl (light blue), #169069: $CaAl_2O_4$ (blue), #169073: Li_2TiO_3 (red).

Figure 3 shows a plasma waveform summary for four(4) high-density (a line-averaged electron density n_{e_bar} of 4-5 x 10^{19} m^{-3}) LHD plasmas, #169063: SiB_6 (orange), #169067: NaCl (light blue), #169069: $CaAl_2O_4$ (blue), #169073: Li_2TiO_3 (red). The target plasmas with the high-density are also almost identical. After the TESPEL injection, the line-averaged electron density was also slightly increased. Then the elevated line-averaged electron density was decreased to the pre-injection level again. The decay times of the line-averaged electron density seems to be longer than those in the low-density case. The change in the central electron temperature due to the addition of NBI#4 and NBI#5 seems to be weaker and slower than that in the low-density case. This is because heat deposition profiles by NBI#4 and NBI#5 become very hollow in the high-density plasmas. Figure 4 (a-c) shows temporal evolutions of the CX Li III, CX B V, and CX Al XIII emissions measured with the CXS technique in the high-

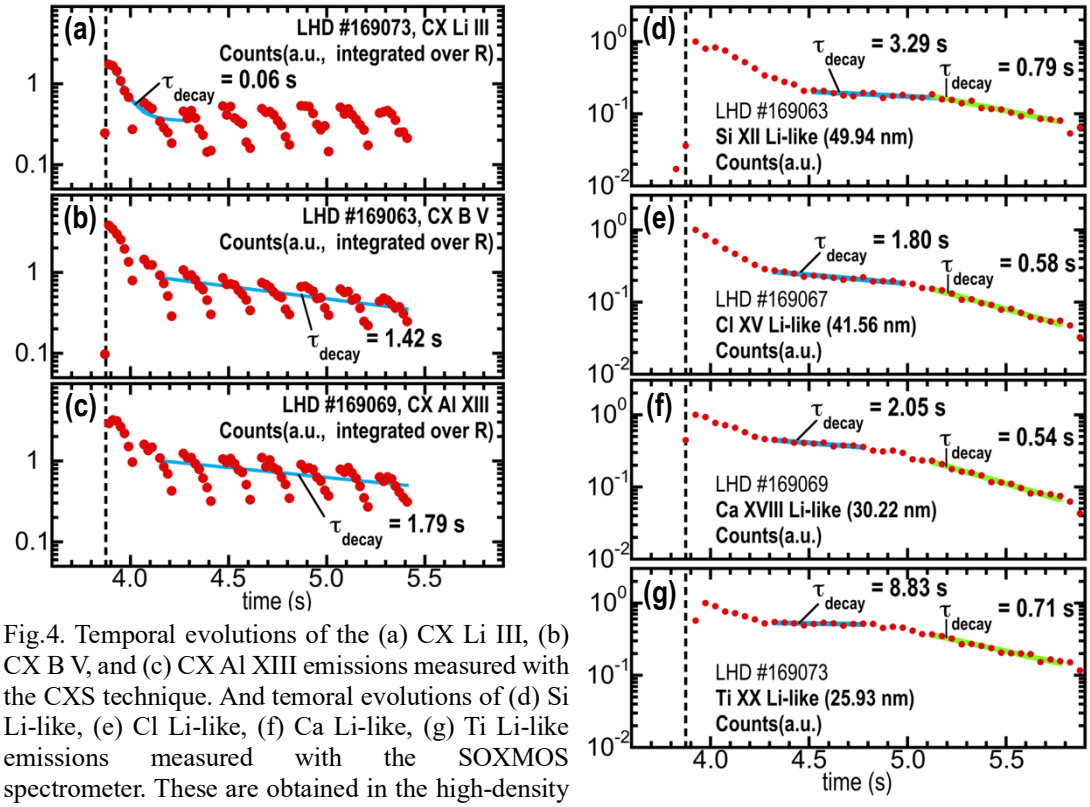

Fig.4. Temporal evolutions of the (a) CX Li III, (b) CX B V, and (c) CX Al XIII emissions measured with the CXS technique. And temoral evolutions of (d) Si Li-like, (e) Cl Li-like, (f) Ca Li-like, (g) Ti Li-like emissions measured with the SOXMOS spectrometer. These are obtained in the high-density LHD plasmas. The vertical dashed line indicates the TESPEL injection time. All the Li-like emissions are normalized by the maximum druing the time period shown.

density plasmas. All the CX emissions were again increased clearly in response to the TESPEL injection. However, the decay times of CX emissions from B, and Al ions become much longer than those in the low-density case. On the other hand, the decay time of CX Li III emissions in the high-density plasma was found to be almost the same as that in the low-density. Figure 4 (d-g) shows temporal evolutions of Li-like emissions from Si, Cl, Ca, and Ti ions in the high-density plasmas. The temporal behaviours of Si, Cl, Ca, and Ti Li-like emissions indicate that there are three (3) phases in those behaviours. The temporal behaviours just after the TESPEL injection are defined as the first phase. In this phase, the impurities introduced into the LHD plasmas by the TESPEL are being distributed in the plasma. And then, the temporal behaviour of Si, Cl, Ca, and Ti Li-like emissions show little change (2nd phase). The decay times estimated in the 2nd phase become much longer, compared to the other phase and the decay time in low-density plasmas. In this phase, the impurities seem to accumulate in the core region of LHD plasma. However, at the time of around 5.0 s, the temporal behaviours of Li-like emissions have changed, and all the Li-like emissions restarted to decay. In other words, the impurity accumulation seems to disappear at the time of around 5.0 s. The reasons why the impurity behaviours show 3 phases remains unclear. The impurity transport time as a function of atomic number (Z) for both the low- and high-density cases is summarized in Fig. 5. In the low-density case, the impurity transport times seem to increase linearly. The impurity transport times, which are taken from the 2nd phase of those temporal behaviours, in the high-density case is an order of magnitude higher than that in the low-density case. But there seems to be no clear dependence of the impurity transport time on the atomic number.

Summary A new type of TESPEL, which contain the inorganic compound, has been utilized for investigating the Z-dependence of core impurity transport in the LHD plasmas. Thanks to the new type of the TESPEL, line emissions from both lower- and higher-Z impurity ions were successfully observed with the charge exchange spectroscopic technique and the EUV spectrometer. We estimated a transport time of each impurity, from Li (Z = 3) to Ti (Z = 22), injected by the TESPEL in both low- and high-density NBI-heated LHD plasmas. The estimated transport time for the low-density LHD plasmas seems to increase with the atomic number (Z). However, the dependence of estimated transport time for the high-density LHD plasmas on the atomic number was not clear. This would be explained by the non-monotonic decay features of the impurity line emissions observed in the high-density plasmas. As future work, the monotonic temporal behaviours of the impurity line emissions should be obtained in the high-density regimes for acquiring the general Z-dependence of the core impurity transport in the LHD plasmas.

Acknowledgements We would like to thank the LHD experiment group and the technical staff of LHD for their effort to support the experiment in LHD. This work was supported by a JSPS KAKENHI JP19H01881 and a budgetary Grant-in-Aid (Grant Nos. ULHH007 and ULHH012) of the National Institute for Fusion Science.

References

[1] S. Sudo, J. Plasma Fusion Res. **69**, 1349 (1993)., [2] N. Tamura et al., Rev. Sci. Instrum. **92**, 063516 (2021)., [3] N. Tamura et al., submitted to JINST.

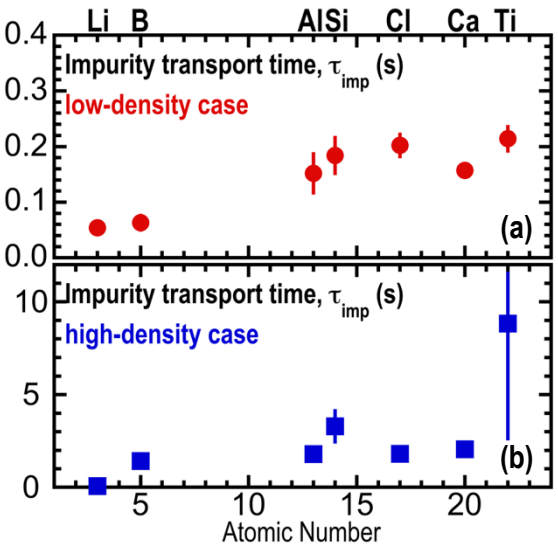

Fig.5. Impurity transport time, τ_{imp} as a function of atomic number for (a) the low-density case and (b) the high-density case.